International Communications in Heat and Mass Transfer 85 (2017) 100–106

Contents lists available at ScienceDirect

International Communications in Heat and Mass Transfer

journal homepage: www.elsevier.com/locate/ichmt

A two-dimensional simulation method of the solar chimney power plant with a new radiation model for the collector

Ming-Hua Huang[a], Lei Chen[a], Ya-Ling He[a], Jun-Ji Cao[b], Wen-Quan Tao[a,*]

[a] Key Laboratory of Thermo-Fluid Science and Engineering of MOE, Xi'an Jiaotong University, Xi'an 710049, China
[b] Key Laboratory of Aerosol, SKLLQG, Institute of Earth Environment, Chinese Academy of Sciences, Xi'an 710061, China

ARTICLE INFO

Keywords:
Solar chimney power plant
CFD
Two dimensional axisymmetric model
Solar radiation
Radiation heat transfer
Greenhouse effect

ABSTRACT

A two-dimensional axisymmetric CFD method is proposed for the solar chimney power plant (SCPP), which includes a solar radiation model within the collector, an energy storage model, an air flow and heat transfer model, and a turbine model. Numerical simulation is conducted for the Manzanares pilot plant. Different solar radiation modes in the collector and simulation methods are compared and discussed. Results show that the present two-dimensional method obtains consistent results with the three-dimensional method in the literature and experiment data, validating the feasibility of the proposed two-parallel-plate model for the radiation heat transfer within the collector.

1. Introduction

A solar chimney power plant (SCPP) mainly consists of a solar collector, a chimney and a turbine as shown in Fig. 1. The world's first SCPP was built in Manzanares, Spain, in 1981 and ran successfully seven years. The SCPP has no pollution to the environment and operates without auxiliary energy. These advantages have been drawing an ever increasing research attention, especially in recent years in the context of energy crisis and environment deterioration.

Since Haaf et al. [1,2] presented the principle and constructing of the pilot plant in Manzanares and later described the preliminary test results in 1984, a large amount of studies, including experimental, analytical and numerical have been reported. Some experimental prototypes have been presented in [3–8]. Experimental model study can provide test data which are useful for further understanding the physical process and can be used for validation of numerical models. However, in some sense it is prohibited because of the large consumptions in human resource, money and time. Early in the nineties of the last century, a thermal equilibrium method on the basis of the first law of thermodynamics was presented to analyze the performance of the SCPP, coupled with walls and thermal updraft air thermal equilibrium equations [9]. Since then several studies [10–14] developed different theoretical analyses and mathematical models to predict the efficiency, outlet air velocity and power output for the SCPP. Analytical method is simple and can provide a quick result such as system efficiency, but often is limited by its assumptions and cannot provide the details of physical process in the entire system. In the recent ten years, many studies used computational fluid dynamics (CFD) methods to simulate the flow and heat transfer in the SCPP and predict the output power on the basis of solving coupled mass, momentum and energy equations. Post-processing of simulation data can visually describe the flow and temperature of the SCPP in detail. Pastohr et al. [15] conducted a 2D steady numerical simulation for the Manzanares pilot plant by commercial software Fluent. After then, many papers proceeded to simulate the SCPP by adopting software Fluent.

The SCPP system is a multi-physics coupling system. The entire simulation model of the SCPP can be divided into four sub-models: the solar radiation model, the energy storage model, the air flow and heat transfer model, and the turbine model. In previous studies, solid model [15], porous model [16] and phase change model [17] have been proposed for the energy storage simulation. The air flow and heat transfer in a SCPP is a typical incompressible convective heat transfer induced by buoyancy force. This process can be simulated by many available commercial software, and Fluent is widely adopted. What's more Boussinesq approximation is always used to consider the change of air density with temperature [16,18,19,20,21], because temperature difference in the SCPP is small. For the turbine simulation, at present most papers adopt a pressure jump model in Fluent [19,21,22]. The major differences of the related papers adopted Fluent is the radiation model.

In the previous studies, there are three different modes taking solar radiation into consideration. The first mode sets the solar radiation as the boundary conditions, say, a heat source in a 0.1 mm-thickness ground surface, and a certain temperature or heat flux profile on the

* Corresponding author.
E-mail address: wqtao@mail.xjtu.edu.cn (W.-Q. Tao).

http://dx.doi.org/10.1016/j.icheatmasstransfer.2017.04.014

Available online 18 May 2017

Nomenclature

A	area (m^2)
c_p	specific capacity ($J\,kg^{-1}\,K^{-1}$)
E	energy (J)
h	convection heat transfer ($W\,m^{-2}\,K^{-1}$)
I	solar radiation ($W\,m^{-2}$)
J	effective radiation ($W\,m^{-2}$)
m	mass flus ($kg\,s^{-1}$)
P	power (W)
P_{gage}	gage pressure (Pa)
Q	volumetric heat source ($W\,m^{-3}$)
Q_v	volume flow rate ($m^3\,s^{-1}$)
q	heat flux ($W\,m^{-2}$)
R	radius (m)
Ra	Rayleigh number (−)
T	temperature (K)
T_{sky}	equivalent temperature of the sky (K)

Greek symbols

α	absorptivity (−)
ε	emissivity (−)
λ	wave length
ρ	density ($kg\,m^{-3}$)
σ	Stefan-Boltzmann constant ($W\,m^{-2}\,K^{-4}$)
μ	dynamic viscosity ($N\,s\,m^{-2}$)
τ	transmittance (−)
Δ	difference (−)
δ	thickness (m)

Subscripts

a	ambient
b	the bottom of the collector
c	collector
t	the top of the collector/turbine

ground surface. There are two ways for implementing this mode. The first method of this mode [15,23,24] is the simplest which does not take the collector canopy into consideration and takes 0.1 mm thin layer of the ground surface absorbing all the solar radiation (Fig. 2a). The second method of this mode [18,25] simply considers the collector canopy absorption and transmission of solar short-wave radiation (named as τ-α model, Fig. 2b). It can be seen that the two methods do not consider the greenhouse effect of the collector. The 2nd mode was adopted in Koonsrisuk and Chitsomboon's study [26], where solar energy is treated as volume heat source of air within the airflow in the collector. It should be noted that according to heat transfer theory [27,28] air is a transparent medium and does not participate radiation heat transfer. Thus this mode might be simple but conceptually incorrect. The 3rd mode applies the solar ray tracing model and the DO radiation model in Fluent by Guo et al. [19] and Gholamlizadeh and Kim [22]. Their results both show a decline on the updraft velocity and the whole output power, and are closer to the measured data compared with relative previous studies. Compared with former two modes, Mode 3 is more reasonable and practical. Because Mode 3 considers the greenhouse effect in the collector resulted from the spectral radiative properties of the semi-transparent canopy and energy storage layers. Taking glass for example, a clear glass can transmit almost 90% radiation for $\lambda < 2.5\,\mu m$, but is nearly opaque for $\lambda > 2.5\,\mu m$. Solar radiation is substantially in the range of 0.29–2.5 μm, and radiation wave length emitted by the ground is mainly in the range of 3–120 μm [28]. So about 96% solar energy can arrive in the ground, and the ground radiation can barely transmit through the glass to the ambient. Thus in the radiation model taking the greenhouse effect into consideration is very important for appropriate simulation of the SCPP. Nevertheless, it must be pointed that in Fluent the solar ray tracing model is only available for 3D simulation, and even for the steady state simulation the 3D method is very time-consuming. Considering the fact that a real SCPP usually has huge geometric configuration, it is very attractive that if a 2D model can be established in which the radiative effects can also be taken into account with enough accuracy. In addition a 2D model will make the unsteady state simulation much less expensive than a 3D model.

In this paper, we propose an improved 2D model for SCPP simulation. The simulation model is consisted of four sub-models as indicated above. The major contribution of this paper is the improvement of the solar radiation model, which can take the spectral property of the collector into account and is named as Mode 4. This new radiation model is self-coded and combined with Fluent 14.0 in ANSYS as UDFs. This improved 2D method is used to simulate the Manzanares pilot plant, and good agreement between the measured and predicted results is obtained. The improved 2D method overcomes the overestimation for the SCPP performance of previous methods and has similar results to the 3D method with the solar ray tracing model and the DO radiation model with much less computational efforts.

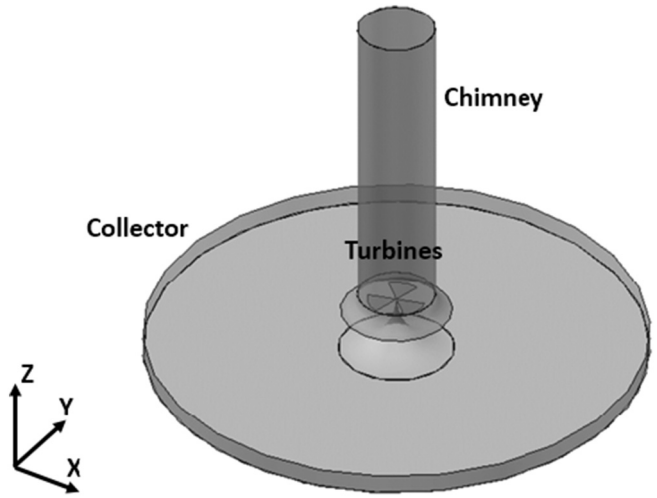

Fig. 1. Structure sketch of the SCPP.

2. Numerical methods

In order to simplify the calculation while still keep the major features of an SCPP, the following assumptions are made in simulations:

(1) The solar irradiation is constant and uniform.
(2) The soil temperature 5 m underneath the ground surface is set to be 300 K and is taken to be as the boundary condition.
(3) When the radiation heat transfer between collector top and bottom is considered the collector is treated as a two-parallel- plate system.
(4) Radiation surfaces are all diffuse-grey surfaces.
(5) The heat loss of the chimney wall is negligible.
(6) Boussinesq approximation is used to account for the change of air density.
(7) The environment is static.
(8) The process is in the steady state.

2.1. Mathematical models

In an SCPP, the strength of the buoyancy-induced flow is measured

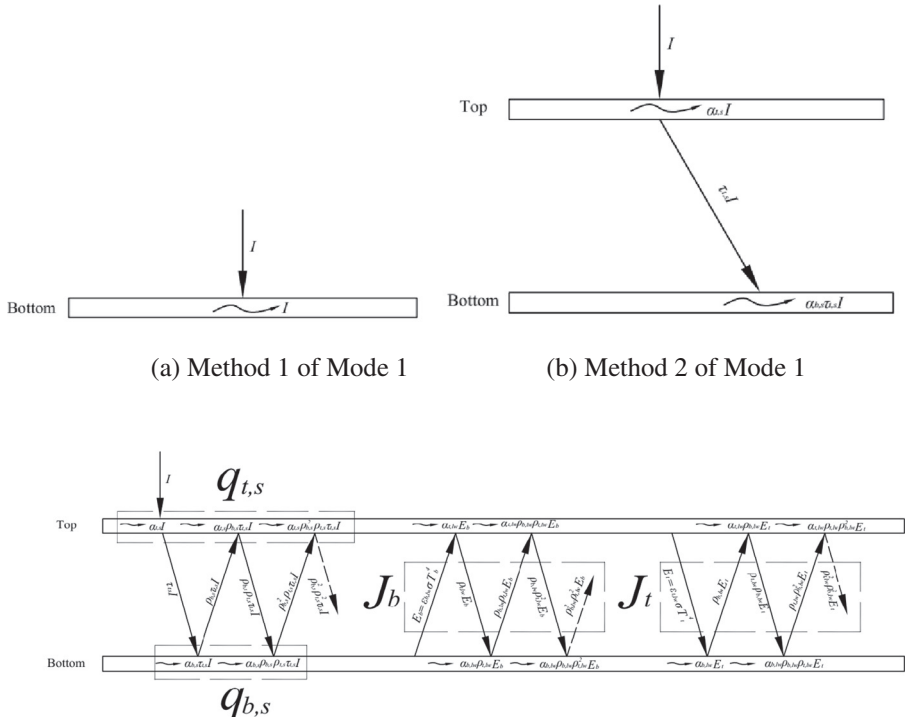

Fig. 2. Mode 1 and the proposed mode (Mode 4) of radiation heat transfer in the collector.

by the Rayleigh number. In the collector and chimney of the Manzanares pilot plant, the *Ra* numbers are both $> 10^{10}$, therefore, air flow through the SCPP system is the turbulent flow. The standard *k-ε* model is employed to simulate the turbulent flow. By simplifying the 3D problem to a 2D axisymmetric one, the governing equations of coupled mass, momentum and energy equations can be solved by ANSYS Fluent14.0 [29] in 2D cylindrical coordinates.

For the compacted soil, there is little difference between the solid model and the porous model. So the ground is taken as a solid zone and the thickness is 5 m that is sufficient for taking as bottom boundary. The temperature governing equation of the soil is the energy equation which can also be solved by ANSYS Fluent14.0 [29].

The solar radiation is assumed to be constant and uniform when it reaches the outside surface of the collector. However, when it goes into the inner space of the collector complicated energy exchange between the top inner side and the ground surface happens which is three dimensional in nature. Since the collector radius is much larger than the distance between its top and bottom, we can simplify the top and bottom as two parallel infinite plates which makes the exchange problem to be two-dimensional. For engineering application, such simplification and assumption are reasonable and acceptable. It is this reasonable assumption that makes the simulation two-dimensional.

As described above, in the study of solar chimney power plant three radiation modes have been used. This paper presents the 4th mode that not only considers the solar short-wave radiation (defined as radiation with wave length equal to and < 2.5 μm) but also the ground surface long-wave radiation (defined as radiation with wave length within 3–120 μm), meanwhile computation is limited in 2D. Thus its accuracy is much higher than the 1st simple mode, while its computational cost is much less than the 3rd complicated mode. Followings are the major contents of this new mode.

As shown in Fig. 2c, the net heat flux absorbed from sun radiation by the top and the bottom can be expressed as an infinite geometric series and converges to [27,28]:

$$q_{t,s} = \left(1 + \frac{\tau_{t,s}\rho_{b,s}}{1 - \rho_{b,s}\rho_{t,s}}\right)\alpha_{t,s} I \tag{1}$$

$$q_{b,s} = \frac{1}{1 - \rho_{b,s}\rho_{t,s}}\alpha_{b,s}\tau_{t,s} I \tag{2}$$

where the first subscript stands for the collector wall, and *t* and *b* indicate the collector top inner side wall and the bottom wall, respectively. The second subscript *s* means the radiation emitted from sun. Table 1 displays $q_{t,s}$ and $q_{b,s}$ in Mode 1 and Mode 4.

Meanwhile, the long-wave radiations are emitted from the collector top wall and the bottom wall. Formulas of effective radiation at the collector top and bottom can be expressed as [27,28]:

$$J_t = \frac{E_t + \rho_{t,lw}E_b}{1 - \rho_{t,lw}\rho_{b,lw}} \tag{3}$$

$$J_b = \frac{E_b + \rho_{b,lw}E_t}{1 - \rho_{t,lw}\rho_{b,lw}} \tag{4}$$

where the subscript *lw* represents the long-wave radiation emitted from the collector inner side top wall and the bottom wall. J_t,J_b will be used later to determine the volumetric heat source of the collector top and bottom resulted from solar radiation.

Essentially, Mode 1 and Mode 4 both add the solar load as heat source to the collector boundary zones, then the convective heat transfer between air and the boundary increases air temperature in the collector. Another common method makes solar load as heat source of air in the collector, like Mode 2. As mentioned above Mode 2 is

Table 1
Solar radiation absorbed by the top and bottom of the collector.

Type	$q_{t,s}$ (W/m^2)	$q_{b,s}$ (W/m^2)
Method 1 of Mode 1	0	800.00
Method 2 of Mode 1	32.00	588.80
Mode 4	37.94	593.55

conceptually incorrect. However, very recently some literatures still claimed or vaguely wrote that incident solar radiation is treated as a heat source term in the air flow energy equation in the SCPP simulation, like Ref. [22]. Later in this article, the four solar radiation modes will be compared and the irrationalities of Mode 2 will be pointed out.

2.2. Boundary conditions and numerical procedure

In this study, the physical model is based on the Manzanares pilot plant. Main dimensions are listed in Table 2. The computational domain is shown in Fig. 3, where a soil layer under the bottom of the collector is a part of the domain. Table 3 shows the boundary conditions of the computational domain. For the collector cover, the convective heat transfer coefficient is calculated based on Bernardes et al.'s study [30] and T_{sky} is the external radiation temperature that can be represented as [31]:

$$T_{sky} = 0.0552 T_a^{1.5} \tag{5}$$

where T_a is the ambient temperature.

For the turbine, the pressure drop values across the turbine are 80 Pa at the solar radiation of 800 W/m^2 and 70 Pa at the solar radiation of 850 W/m^2 according to the measured data of the Manzanares pilot plant on 2 September 1982 [2].

In Table 3, Q_3, Q_4 are the volumetric heat sources of the collector top and bottom walls resulted by solar radiation respectively, and are loaded and updated every iteration by UDFs. They can be determined by following equations:

$$Q_3 = (q_{t,s} + \alpha_{t,lw} J_b - E_t)/\delta_t \tag{6}$$

$$Q_4 = (q_{b,s} + \alpha_{b,lw} J_t - E_b)/\delta_b \tag{7}$$

where δ_b indicates the thickness of the thin energy storage layer on the ground surface taken equal to 0.1 mm, and δ_t means the collector cover thickness taken equal to 5 mm.

In this paper, a standard k-ε model, and the standard wall functions in the Fluent were selected. Self-programmed UDFs were loaded in the boundary conditions. When starting the simulation, the temperatures of the collector cover and bottom were assumed, then before every iteration, the temperatures of the collector cover and bottom were read and thermal equilibrium equations were computed to redistribute the heat sources in the top cover glass and the bottom, respectively. The SIMPLE algorithm was applied and the second-order upwind scheme was selected for discretization of the convective terms in momentum and energy equations. Meanwhile, the grid independence of numerical solutions was verified. The final total number of grids is 116,889 cells. The distance from the first layer grids to the wall is sufficiently small to guarantee that the Y^+ is in the range of 30 to 300. Physical properties of top cover glass and soil are shown in Table 4.

3. Results and discussion

3.1. Comparison of solar radiation Mode 1, Mode 2, Mode 3 and Mode 4.

In order to only compare the solar radiation modes in the collector, all simulations in this section were implemented with the same other sub-models except the solar radiation mode at no-load condition (i.e., no power is generated).

Firstly, Mode 1 and Mode 4 are compared at the incident solar radiation of 800 W/m^2.

The collector efficiency η_c is the key parameter to estimate the overall efficiency of the SCPP that can be determined by [19]:

$$\eta_c = \frac{c_p m \Delta T}{\pi R_c^2 \cdot I} \tag{8}$$

where m and ΔT denote mass flow rate and air temperature rise in the collector, respectively.

Fig. 4 shows the collector efficiency of the SCPP by Mode 1 and Mode 4. Method 1 of Mode 1 has the highest collector efficiency. Because heat flux absorbed by the ground of Method 1 of Mode 1 is the highest (see Table 1). Method 1 of Mode 1 assumes that the irradiation of the solar energy is absorbed completely by the ground surface, leading to an overestimation of the received solar radiation of the SCPP. By considering the spectral radiation properties of glass and soil in Method 2 of Mode 1 and Mode 4, the ground absorbed heat flux greatly decreases. The difference between Method 2 of Mode 1 and Mode 4 is as follows: the former only pays attention to the short-wave radiation of the sun, while Mode 4 fully considers the short-wave radiation and the long-wave radiation in the collector. In Mode 4 ground long-wave radiation is absorbed by the glass and then part of it is transferred to the environment that causes to some energy losses to the ambient. So Mode 4 has the minimum collector efficiency. Temperature profiles of the ground surface of Mode 1 and Mode 4 also show the overestimation in the collector efficiency of Mode 1. As shown in Fig. 5, the three temperature profiles have the same variation pattern, but temperatures of Mode 1 have higher values than those of Mode 4. The higher ground temperature will lead to a larger mass flow rate and air temperature rise. So neglecting the greenhouse effect in the collector in Method 1 and 2 of Mode 1 will result in overestimating the ground surface temperature and the collector efficiency of the SCPP.

Secondly, Mode 2 and Mode 4 are compared. As already mentioned, Mode 2 adopted in [26] sets the absorbed solar energy as heat source to the air energy equation in the collector. In this paper we only treat the short-wave radiation energy of the sun as a heat source term of the air energy equation in Mode 2. So in the simulation of Mode 2, we uniformly assigned the sum of short-wave solar radiation absorbed by the collector top and bottom as shown for Mode 4 in Table 1 to every computational cell of air flow in the collector. Meanwhile, the long-wave radiation in the collector is considered in collector boundary zones by UDFs in Fluent, like Mode 4. Fig. 6 illustrates the cross-section temperature distributions of air in the SCPP. Obviously, temperatures of the soil heat storage layer in Mode 4 are much larger than those in Mode 2. And the most important finding of this comparison is that the temperature of ground surface is higher than the air temperature in the collector in Mode 4 which is physically meaningful, but, on the contrary, in Mode 2 the air temperature in the collector is higher than the ground surface, which physically cannot be accepted. Thus even though Mode 2 accords with the energy conservation in total, the predicted temperature distribution by this mode is physically incorrect.

Finally, 3D Mode 3 and 2D Mode 4 are compared. According to Gholamalizadeh et al.'s study [22] which adopts the solar radiation Mode 3 by Fluent the predicted velocity of the chimney inlet and the collector temperature rise are 11.4 m/s and 14 K, respectively, at no-load condition and at the solar radiation of 850 W/m^2. The relevant results predicted by the present method are 11.9 m/s and 13.5 K, respectively. Thus the present 2D method can obtain results very agreeable with those by 3D methods (including flow fields and radiation) with much less computational effort.

3.2. Comparison of the present method with methods in other literatures

Pasumarthi et al. [9], Pastohr et al. [15], Ming et al. [16], and

Table 2
Main dimensions of the physical model.

Parameter	Value
Mean collector radius	122 m
Mean collector height	1.85 m
Chimney height	194.6 m
Chimney radius	5.08 m
Turbine height	9 m
Ground thickness	5 m

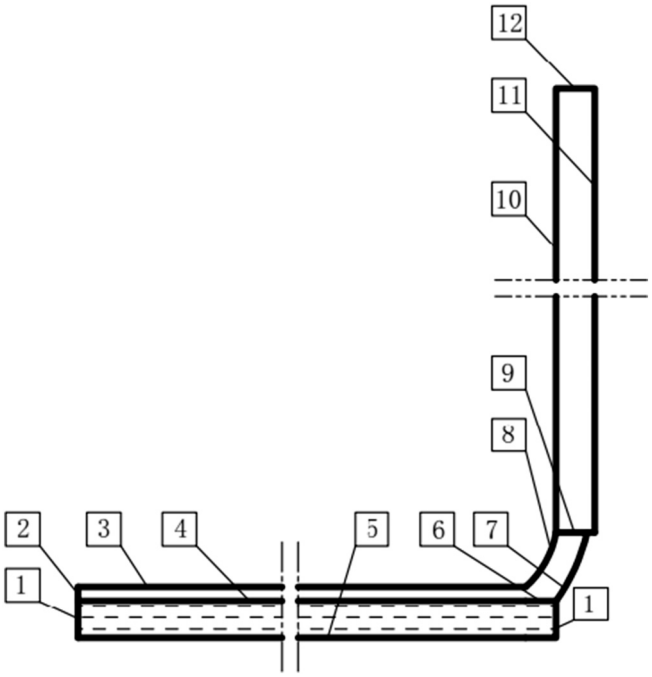

Fig. 3. The computational domain.

Table 3
Boundary conditions for the computational domain.

Place	Type	Value
1,7, 8,10	Adiabatic wall	$q = 0$ W/m^2
2	Pressure inlet	$P_{gage} = 0$ Pa, $T_a = 300$ K
3	Mixed Wall	$h = 6$ W/(m^2 K), $T_a = 300$ K, $T_{sky} = 286.83$ K, Q_3
4	Couple wall	Q_4
5	Temperature wall	$T = 300$ K
6	Couple wall	/
9	Reverse fan	Measured data
11	Axis	/
12	Pressure outlet	$P_{gage} = 0$ Pa

Table 4
Physical properties of materials.

Physical property	Glass	Soil
Density (kg m^{-3})	2700	1900
Specific heat (J kg^{-1} K^{-1})	840	2200
Thermal conductivity (W m^{-1} K^{-1})	0.78	1.83
Absorption coefficient	$\alpha_{t,s} = 0.04$ $\alpha_{t,lw} = 0.90$	$\alpha_{b,s} = 0.80$ $\alpha_{b,lw} = 0.80$
Transmission coefficient	$\tau_{t,s} = 0.92$ $\tau_{t,lw} = 0.05$	$\tau_{b,s} = 0$ $\tau_{b,lw} = 0$
Emissivity	0.90	0.80

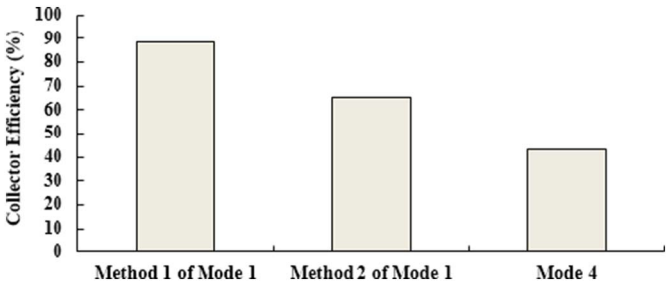

Fig. 4. Collector efficiencies by Mode 1 and Mode 4.

Gholamalizadeh et al. [22] all have simulated the Manzanares pilot plant under the loaded working state at solar radiation of 800 W/m^2, and Haaf et al. [2] gave the test results under these conditions in 1984. In above four simulation studies, the simulation approaches and models are different. The Pasumarthi et al.'s method is a one-dimensional energy equivalent method and puts the solar radiation into the source term of air energy equation, like Mode 2. Pastohr et al.'s and Ming et al.'s methods are 2D CFD methods, and for the solar radiation model, Pastohr et al. adopted Method 1 of Mode 1 and Ming et al. simulated the radiative heat transfer in the collector without considering the spectral radiative properties of the semi-transparent canopy and energy storage layers. The above three methods all ignore the greenhouse effect in the collector. The Gholamalizadeh et al.'s method employs the 3D solar ray tracing model and DO radiation model (radiation Mode 3). Ref. [22] has compared the four methods, and in this section, the results of the present method (Mode 4) will join in the comparison.

Fig. 7 compares the ground surface temperature profiles calculated by the present method and the above-mentioned methods. According to the data measured in Manzanares pilot plant, the maximum temperature of the ground surface at the middle of the collector was 348 K when the solar irradiation is about 800 W/m^2 [2]. Pastohr's and Ming's results are much larger than the measured value. Pasumarthi's result is lower than the previous two but is still appreciably higher than the measured value. The ground surface temperature profile gained by the present method is very close to the Gholamalizadeh's profile, and the maximum deviation is about 10% at a distance of about 10 m near the collector inlet. The maximum temperature is 352 K obtained by the Gholamalizadeh et al.'s method and the predicted value of this temperature is 351 K by the presented method only 3 K above the experimental value. The gross overestimation on the ground surface temperature without considering the greenhouse effect will lead to the temperature rise of air flow in the collector, hence, leading to some exaggeration of the system flow rate. The formula of the SCPP power output can be expressed as [19]:

$$P = \eta_t \times \Delta P_t \times Q_v \tag{9}$$

where η_t is the turbine efficiency,ΔP_t is the turbine pressure drop, Q_v is the volume flow rate. Thus the power output will be overestimated with exaggerated system flow rate. From Eq. (9) it can also be seen that the comparison of numerical results with test data may be conducted just for airflow rate (or the upwind velocity in the chimney) with the measured turbine pressure drop as input data, but not for SCPP power output for which the selection of turbine efficiency is quite arbitrary.

Haaf et al. [2] showed that ΔT generated by the collector was 17.5 K and the upwind velocity was 8.8 m/s with the irradiation of 850 W/m^2 at midday on 2 September 1982. Some research [19,22] simulated this case, but applied different turbine pressure drop according different analytical method. In this paper, we adopted 70 Pa that is the measured pressure drop in the turbine on that day. Our simulation results show that the collector temperature difference and the upwind velocity in the chimney are 18.2 K and 9.7 m/s, respectively, which deviate from the test data by 4% and 10.2% respectively. So the present 2D method with improved solar radiation model which takes the greenhouse effect into account can provide a reliable estimation for the SCPP.

4. Conclusions

For the purpose of developing an accurate and efficient simulation method for an SCPP, 2D axisymmetric steady numerical simulations have been performed for the Manzanares pilot plant by ANSYS Fluent 14.0 with authors-coded UDFs for radiation heat transfer within the collector. Different radiation modes are compared. Numerical results of the present 2D method are in good agreement with those of 3D method and test data of the pilot plant. The major conclusions are as follow:

(1) Neglecting the greenhouse effect in the collector will overestimate

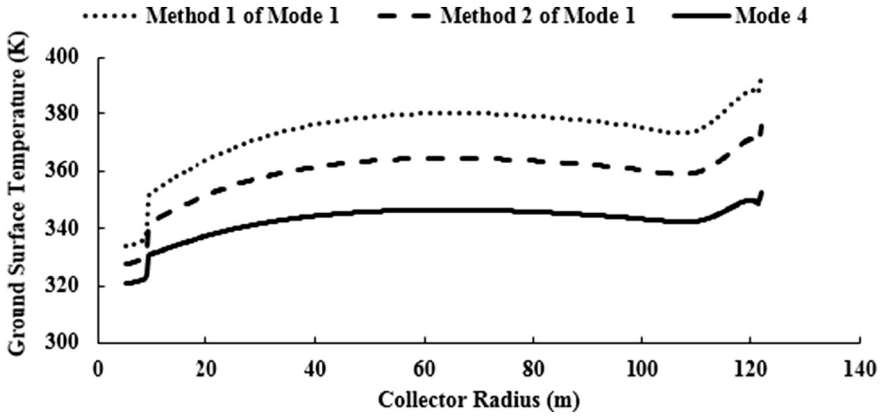

Fig. 5. Temperature profiles of the ground surface by Mode 1 and Mode 4.

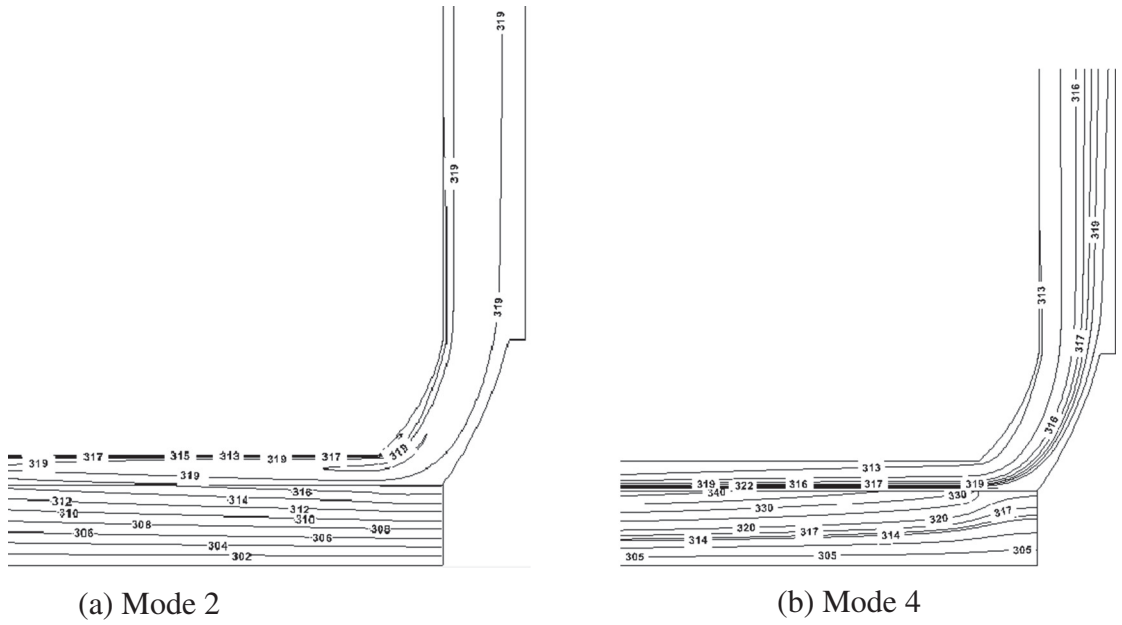

Fig. 6. Cross-section temperature distributions of the SCPP by Mode 2 and Mode 4.

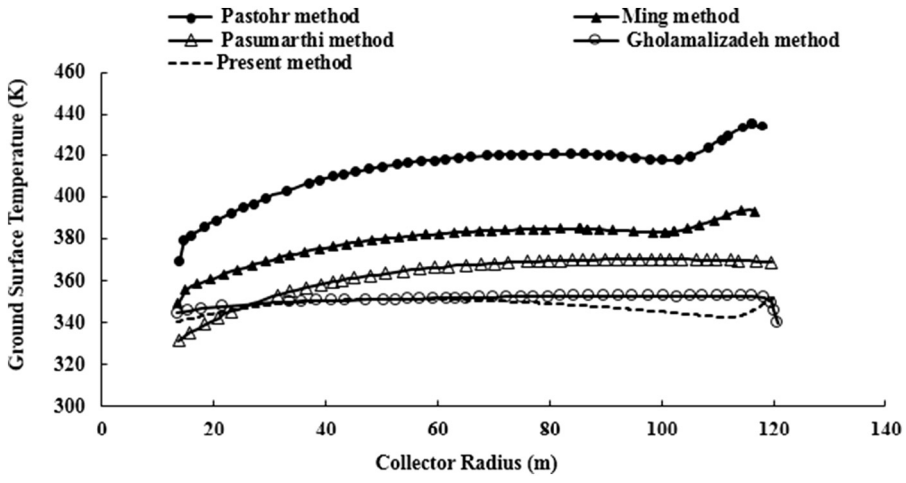

Fig. 7. Temperature profiles of the ground surface by different methods.

the collector efficiency, the ground surface temperature and the power output of the SCPP.

(2) While adding the energy of the absorbed solar radiation into the air energy equation is consistent with the energy conservation in total, it is conceptually incorrect and leads to overestimated air temperature distribution in the SCPP.

(3) The good agreement of numerical results of the present 2D model with those of 3D model in conjunction with solar ray tracing model

and DO radiation model and with the experimental data validates the proposed two-parallel-plate radiation heat transfer mode within the collector.

Acknowledgements

The authors would like to acknowledge the support provided by the Key Project of National Natural Science Foundation of China (Grant No.51436007),the 111 Project (B16038) and the Key Research Program of the Chinese Academy of Sciences (Approved on 8 August, 2014).

References

[1] W. Haaf, K. Friedrich, G. Mayr, J. Schlaich, Solar chimneys - part I: principle and construction of the pilot plant in Manzanares, Int. J. Sol. Energy 2 (1983) 3–20.
[2] W. Haaf, Solar chimneys, Int. J. Sol. Energy 2 (1984) 141–161.
[3] R.J.K. Krisst, Energy transfer system, Altern. Sources Energy 63 (1983) 8.
[4] H. Kulunk, A prototype solar convection chimney operated under Izmit conditions, Proceedings of the 7th Miami International Conference on Alternative Energy Sources, vol.162, 1985.
[5] N. Pasumarthi, S.A. Sherif, Experimental and theoretical performance of a demonstration solar chimney model – PartII: experimental and theoretical results, Int. J. Energy Res. 461 (1998) 443–461.
[6] X. Zhou, J. Yang, B. Xiao, G. Hou, Experimental study of temperature field in a solar chimney power setup, Appl. Therm. Eng. 27 (2007) 2044–2050.
[7] A.B. Kasaeian, E. Heidari, S.N. Vatan, Experimental investigation of climatic effects on the efficiency of a solar chimney pilot power plant, Renew. Sust. Energ. Rev. 15 (2011) 5202–5206.
[8] L. Zuo, Y. Yuan, Z. Li, Y. Zheng, Experimental research on solar chimneys integrated with seawater desalination under practical weather condition, Desalination 298 (2012) 22–33.
[9] N. Pasumarthi, S.A. Sherif, Experimental and theoretical performance of a demonstration solar chimney model - part I: mathematical model development, Energy 288 (1998) 277–288.
[10] M.A. dos S. Bernardes, A. Voß, G. Weinrebe, Thermal and technical analyses of solar chimneys, Sol. Energy 75 (2003) 511–524.
[11] T.W. von Backström, T.P. Fluri, Maximum fluid power condition in solar chimney power plants - an analytical approach, Sol. Energy 80 (2006) 1417–1423.
[12] X. Zhou, J. Yang, B. Xiao, G. Hou, Simulation of a pilot solar chimney thermal power generating equipment, Renew. Energy 32 (2007) 1637–1644.
[13] J.Y. Li, P.H. Guo, Y. Wang, Effects of collector radius and chimney height on power output of a solar chimney power plant with turbines, Renew. Energy 47 (2012) 21–28.
[14] E. Gholamalizadeh, S.H. Mansouri, A comprehensive approach to design and improve a solar chimney power plant: a special case - Kerman project, Appl. Energy 102 (2013) 975–982.
[15] H. Pastohr, O. Kornadt, K. Gürlebeck, Numerical and analytical calculations of the temperature and flow field in the upwind power plant, Int. J. Energy Res. 28 (2004) 495–510.
[16] T. Ming, W. Liu, Y. Pan, G. Xu, Numerical analysis of flow and heat transfer characteristics in solar chimney power plants with energy storage layer, Energy Convers. Manag. 49 (10) (2008) 2872–2879.
[17] K.E. Amori, S.W. Mohammed, Experimental and numerical studies of solar chimney for natural ventilation in Iraq, Energy Build. 47 (2012) 450–457.
[18] F. Cao, L. Zhao, H. Li, L. Guo, Performance analysis of conventional and sloped solar chimney power plants in China, Appl. Therm. Eng. 50 (2013) 582–592.
[19] P.H. Guo, J.Y. Li, Y. Wang, Numerical simulations of solar chimney power plant with radiation model, Renew. Energy 62 (2014) 24–30.
[20] W.Q. Tao, Numerical Heat Transfer, second ed., Xi'an Jiaotong University Press, Xi'an, China, 2001, pp. 240–243.
[21] Q. Cao, D.Y.H. Pui, W. Lipiński, A concept of a novel solar-assisted large-scale cleaning system (SALSCS) for urban air remediation, Aerosol Air Qual. Res. 15 (2015) 1–10.
[22] E. Gholamalizadeh, M.H. Kim, 3D CFD analysis for simulating the greenhouse effect in solar chimney power plants using a two-band radiation model, Renew. Energy 63 (2014) 498–506.
[23] G. Xu, T. Ming, Y. Pan, F. Meng, C. Zhou, Numerical analysis on the performance of solar chimney power plant system, Energy Convers. Manag. 52 (2) (2011) 876–883.
[24] W. Shen, T. Ming, Y. Ding, Y. Wu, R.K. de-Richter, Numerical analysis on an industrial-scaled solar updraft power plant system with ambient crosswind, Renew. Energy 68 (2014) 662–676.
[25] R. Sangi, M. Amidpour, B. Hosseinizadeh, Modeling and numerical simulation of solar chimney power plants, Sol. Energy 85 (2011) 829–838.
[26] A. Koonsrisuk, T. Chitsomboon, Dynamic similarity in solar chimney modeling, Sol. Energy 81 (2007) 1439–1446.
[27] Y.A. Cengel, A.J. Ghajar, Heat and Mass Transfer: Fundamentals and Applications, fourth ed., MccGraw-Hill, New York, 2011, p. 764.
[28] S.M. Yang, W.Q. Tao, Heat Transfer, fourth ed., Higher Education Press, Beijing, 2006, p. 419.
[29] ANSYS, ANSYS FLUENT 14.0 Theory Guide, ANSYS, Inc., 2014.
[30] M.A. dos S. Bernardes, T.W. von Backström, D.G. Kroger, Critical evaluation of heat transfer coefficients applicable to solar chimney power plant collectors, ISES Sol. World Congr. 2007, ISES 2007, Vol. 3 2007, pp. 1706–1713.
[31] W.C. Swinbank, Long-wave radiation from clear skies, Q. J. R. Meteorol. Soc. 89 (381) (1963) 339–348.